

The Role of Structural Intersubunit Microheterogeneity in the Regulation of the Activity in Hysteresis of Ribulose 1,5-Bisphosphate Carboxylase/Oxygenase¹

Koichi Uemura,^{2,3} Naoki Shibata,^{1,3} Anwaruzzaman,^{2,4} Masumi Fujiwara,² Takashi Higuchi,² Hirokazu Kobayashi,² Yasushi Kai,¹ and Akiho Yokota,^{2,4,5}

¹Plant Molecular Physiology, Research Institute of Innovative Technology for the Earth (RITE), Kizu, Kyoto 619-0292; ²Department of Material Chemistry, Graduate School of Engineering, Osaka University, Suita, Osaka 565-0871; ³Laboratory of Plant Cell Technology, School of Food and Nutritional Sciences, University of Shizuoka-Yada, Yada, Shizuoka 422-8002; and ⁴Graduate School of Biological Sciences, Nara Institute of Science and Technology (NAIST), Ikoma, Nara 630-0101

Received June 29, 2000; accepted July 24, 2000

Many enzymes are composed of subunits with the identical primary structure. It has been believed that the protein structure of these subunits is the same. Ribulose 1,5-bisphosphate carboxylase/oxygenase (RuBisCO) comprises eight large subunits with the identical amino acid sequence and eight small subunits. Rotation of the side chains of the lysine residues, Lys-21 and Lys-305, in each of the eight large subunits in spinach RuBisCO in two ways produces microheterogeneity among the subunits. These structures are stabilized through hydrogen bonds by water molecules incorporated into the large subunits. This may cause different effects upon catalysis and a hysteretic, time-dependent decrease in activity in spinach RuBisCO. Changing the amino acid residues corresponding to Lys-21 and Lys-305 in non-hysteretic *Chromatium vinosum* RuBisCO to lysine induces hysteresis and increases the catalytic activity from 8.8 to 15.8 per site per second. This rate is approximately five times higher than that of the higher-plant enzyme.

Key words: hysteresis, RuBisCO, structural microheterogeneity.

Ribulose 1,5-bisphosphate carboxylase/oxygenase (RuBisCO) [EC 4.1.1.39] catalyzes the CO₂-fixation step of photosynthesis and is the important rate-limiting enzyme of this process (1–3). RuBisCO in most photosynthetic organisms consists of eight large subunits (LS) and eight small subunits (SS) (reviewed in Refs. 4–7). The LS is the catalytic subunit, but the function of the SS remains obscure. The LS is coded by a single gene in the multicopy plastid genome, and the SS are coded by a multigene family in the nuclear DNA (8). The primary structures of the different SS family members are not identical; in spinach RuBisCO, two different SS have an orderly disposition within the holoenzyme (9).

The catalytic activity of RuBisCO is species-dependent

and reflects the atmospheric conditions under which a given species evolved (10, 11). For example, RuBisCOs of higher land plants, which appeared after the atmosphere of the earth became oxygenic, have a higher affinity for CO₂ and a stronger specificity for the carboxylase reaction than for the oxygenase reaction compared to the cyanobacterial enzyme, which appeared in a virtually anoxygenic but carbonated atmosphere (12). Conversely, higher land plant RuBisCOs have lost the ability to catalyze the reaction at the rapid rates shown by the photosynthetic bacterial and cyanobacterial enzymes (4, 13). Furthermore, RuBisCOs of higher land plants are subject to “fallover,” in which, at least *in vitro*, the catalytic rate declines during catalysis to a stationary level (14–18; see also Fig. 5). In contrast, RuBisCOs from algae and photosynthetic bacteria do not show such a loss of activity (19).

“Fallover,” is composed of two components, hysteresis, which occurs during the initial several minutes after the start of the reaction, and a subsequent slow decrease in activity (20). The latter loss of activity is caused by an accumulation of suicide inhibitors formed from the substrate ribulose 1,5-bisphosphate (RuBP) within the catalytic site (15, 18, 20, 21). We have suggested that Lys-21 and Lys-305 in the LS are two of the amino acid residues involved in the conformational change of the RuBisCO protein during hysteresis. These residues are highly conserved among RuBisCOs from higher plants (22), but the corresponding amino acid residues are different in the algal and photosynthetic bacterial enzymes. Binding of the transition state analogue

¹ This work was partly supported by the Petroleum Energy Center subsidized by the Japanese Ministry of International Trade and Industry.

Present addresses: ² Research & Development Center, Unitika Ltd., Uji, Kyoto 611-0021; ³ School of Science, Himeji Institute of Technology, 1497-1 Kaneti, Kamigohri, Ako-gun, Hyogo 678-1200; ⁴ Department of Biochemistry, University of Lincoln, Lincoln, Nebraska, USA.

⁵ To whom correspondence should be addressed: E-mail: yokota@bs.aist-nara.ac.jp

Abbreviations: CABP, 2-carboxyarabinitol 1,5-bisphosphate; ¹⁴C-CABP, [2-¹⁴C]carboxyarabinitol 1,5-bisphosphate; LS, large subunit(s); RuBisCO, ribulose 1,5-bisphosphate carboxylase/oxygenase; RuBP, ribulose 1,5-bisphosphate; SS, subunit(s).

2-carboxyarabinitol 1,5-bisphosphate (CABP) to the catalytic sites of carbamylated or activated spinach RuBisCO induces a similar conformational change to that observed in hysteresis during RuBP carboxylation (19).

The present study re-examines the protein structures near Lys-21 and Lys-305 in the CABP-carbamylated spinach RuBisCO complex using coordinates obtained at 1.8 Å resolution (9), and compares them with those of the carbamylated spinach enzyme (23) and the carbamylated cyanobacterial enzyme–CABP complex (24, 25). We newly found the occurrence of two types of ordered structural microheterogeneity around these amino acid residues among LS with coordinates resolved assuming that all protomers are not identical. The microheterogeneity is suggested to cause two forms of LS to have different carboxylase activities. The involvement of the two lysine residues in hysteresis was then confirmed by site-directed mutagenesis of RuBisCO from the photosynthetic bacterium, *Chromatium vinosum*.

MATERIALS AND METHODS

Materials—Spinach RuBisCO was purified from fresh spinach leaves as reported previously (19). [2-¹⁴C]Carboxyarabinitol 1,5-bisphosphate (¹⁴C-CABP) was synthesized from RuBP and K¹⁴CN (26). RuBP was purchased from Sigma. Other chemicals were of the highest grade commercially available.

Structural Analyses—Structural analyses were conducted by the molecular replacement method using the coordinates deposited in the Brookhaven Protein Data Base. The accession codes are 1RUB, 1AUS, and 1RBL for the quaternary complexes of spinach RuBisCO, carbamylated spinach RuBisCO, and the quaternary complex of *Synechococcus* RuBisCO, respectively.

Site-Directed Mutagenesis and Analyses of RuBisCO—Site-directed mutagenesis was performed as previously described (27) using pCV23, which bears the *rbcA-rbcB* operon from *C. vinosum* (28). To introduce lysine at Arg-21 and Pro-305 in the amino acid sequence of the *Chromatium* enzyme, the codons CGC (bases 37 to 39) and CCG (bases 889 to 891) in the *rbcA-rbcB* sequence were changed to AAA codons sequentially (generating the R21K/P305K double mutant) using the following PCR primers, 5'-GGGCA-TCCAATAGGTCTCTTTGTACTCTTTACGCCCCG-3' and 5'-GAAGTGGATGCCGTGGTGTATTATTGCGGTCGAGCACGGC-3', respectively, where the mutation sites are underlined. All mutations were confirmed by sequencing the entire *rbcA-rbcB* mutant genes with a Shimadzu DNA sequencer, using methods described by the manufacturer.

Escherichia coli JM109 harboring pCV23 and the plasmid bearing mutated *rbcA-rbcB* genes were cultured and wild type and mutant RuBisCOs were purified to homogeneity by previously reported methods (12, 29). Enzyme purity was confirmed by SDS-PAGE (30). The course of the carboxylase reaction was followed by measuring the change in light absorbance of the substrate RuBP at 280 nm (20). The enzymatic properties of RuBisCO were determined by previously described methods (12, 31). The pH of the reaction mixture was 7.5 for the wild type and mutated bacterial RuBisCOs and 8.0 for spinach RuBisCO.

Protein was quantified by the dye-binding assay method (32) with purified spinach RuBisCO as the standard. The

catalytic number of RuBisCO was measured by the ¹⁴C-CABP-binding method (26).

RESULTS

Structural Analyses of Spinach RuBisCO—Each RuBisCO LS has two major domains, an N-terminal domain of mixed α -helices and β -sheets, residues 1 to 150, and a C-terminal domain in the form of an α/β barrel, residues 151 to 475 (33). The catalytic site is at the mouth of the barrel, but residues 60, 65, and 123 from the N-terminal domain of the neighboring LS in the LS dimer (L2 dimer) contribute to the site. The position of Lys-334 at the apex of loop 6 of the α/β barrel is important in polarizing the substrate CO₂, thereby stimulating nucleophilic attack of the C2 carboanion of the enediol of RuBP and/or stabilizing the fixed CO₂ on the transition state intermediate (24, 34). The precise

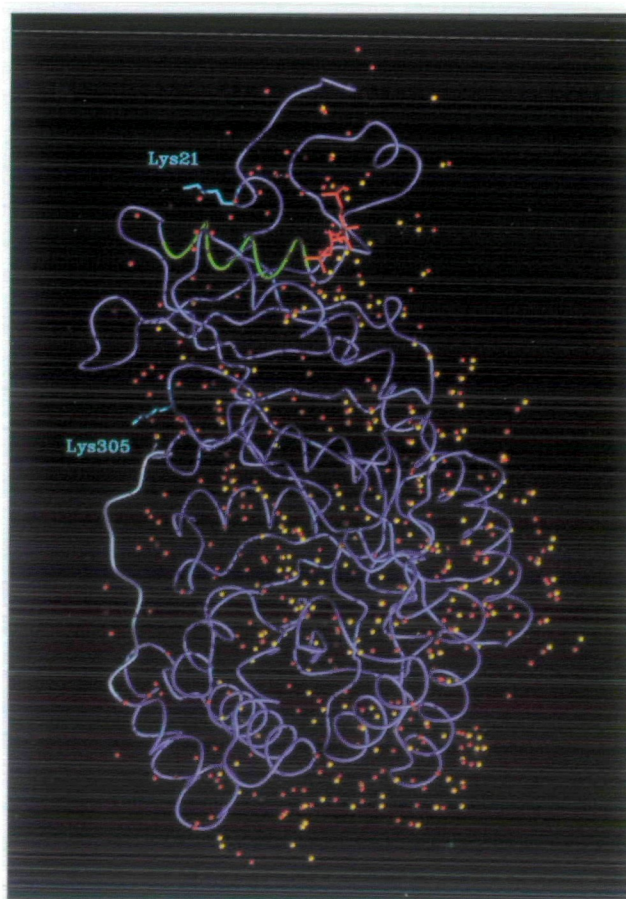


Fig. 1. Locations of Lys-21 and Lys-305 in an LS of the CABP-carbamylated spinach RuBisCO complex and water molecules bound to the carbamylated RuBisCO and the complex. Only the main chain of the LS in the complex is depicted in blue, except Lys-21 and Lys-305 in cyan and the C-terminal sequence from Lys-463 to Val-475 in gray. CABP bound to the catalytic site in the neighboring LS, the structure of which is not depicted, is shown in red. α -Helix B is shown in green. Yellow spheres are water molecules bound to the carbamylated spinach RuBisCO and red spheres are those bound to the CABP-carbamylated RuBisCO complex. The carbamylated holoenzyme binds 1,736 water molecules (B factor < 40 Å²), while 2,412 bind to the CABP-carbamylated complex (B factor < 40 Å²). This figure was drawn with MidasPlus (36, 37).

position of Lys-334 is maintained during catalysis by the carboxyl group of Glu-60, which forms hydrogen bonds with the ϵ -amino group of Lys-334 (34, 35). Lys-21 and Lys-305, which are the focus of the present research, are remote from the catalytic site (Fig. 1).

Re-examination of the coordinates obtained assuming that all protomers of spinach RuBisCO are not identical gave us a chance to notice some amino acid residues with different structures among LS, as in the case of SS (9). In the carbamylated spinach RuBisCO, the side chain of Lys-21 is free (Fig. 2). The carboxyl group of Glu-60 forms hydrogen bonds with the OH group of Tyr-20 and the amide of Asn-123 of the same N-terminal domain. One of the carboxyl oxygens of Glu-52 forms a hydrogen bond with the peptidyl O of the same residue and the other is free. Large structural changes in spinach RuBisCO occur after binding CABP to the carbamylated form (23). Alpha-Helix B, comprising amino acid residues 50 to 60 and the N-terminal Asp-19 to Lys-21, is pulled in about 2 Å toward the catalytic site in the quaternary complex, as reported by Taylor and Andersson (23). The peptidyl N of Tyr-20 and the peptidyl N of Lys-21 form hydrogen bonds with the carboxyl oxygens of Glu-52 in the complex. The carboxyl oxygens of Glu-60 form a hydrogen bond with the OH group of Tyr-20 and a salt bridge with the amino group of Lys-334 in loop 6 from the neighboring LS in a L2 dimer. The amide group of Asn-123 interacts with the carboxyl group of CABP on the catalytic site of the neighboring LS. Thus, the sliding α -helix B is tied at the front and the end of the helix by the N-terminal residues in the quaternary complex. In four of eight LS, the ϵ -amino group of Lys-21 forms a salt bridge with the carboxyl carbon of Asp-19 (the K-D interaction) (Fig. 2). The group is free in the other four LS (see also Fig. 1). The two structures of the side chain result from differ-

ent rotations of the chain between C _{γ} and C _{δ} .

Lys-305 resides in the interface between the N-terminal and C-terminal domains of spinach RuBisCO (Fig. 1). The side chain of Lys-305 in the C-terminal domain forms ionic bonds with carboxyl groups on Glu-93 and Glu-96 in the N-terminal domain of the same LS in the carbamylated form of spinach RuBisCO (K-2E interaction) (23). The C-terminal region 463–475 is free in this conformation. Binding of CABP causes large relocations of hydrogen bonds among the amino-acid side chains around Lys-305. The ϵ -amino group of Lys-305 forms an ionic bond with the OE2 of Glu-93 in the same subunit in four of eight LS in the CABP-carbamylated RuBisCO complex (K-E interaction) (Fig. 3A). The K-E interaction makes a bridge over a large cleft formed between the N- and C-terminal domains. In the remaining four LS, the Lys-305 side chain is rotated between C _{β} and C _{γ} to form an ionic bond with the C-terminal carboxyl oxygen of Val-475 in the same LS (K-OXT interaction).

A LS with the K-E interaction between Lys-305 and Glu-93 always has the K-D interaction between Lys-21 and Asp-19 (Table I). Conversely, a LS with the K-OXT interaction between Lys-305 and Val-475 always has a free Lys-21. The distribution of the heterologous structures is summarized in Fig. 4. The observed microheterogeneity does not seem to cause an energetic imbalance in the LS and destroy the structural stability.

Another major difference between the carbamylated form and the CABP-carbamylated spinach RuBisCO lies in the number of water molecules bound to the enzyme (Fig. 1) (23, 34). When CABP is bound, additional water molecules are found around the α -helix B and Asp-19–Lys-21 region (Figs. 1 and 2), between the C-terminal strand (residues 463 to 475) and loop 6, and in the cleft between the N-ter-

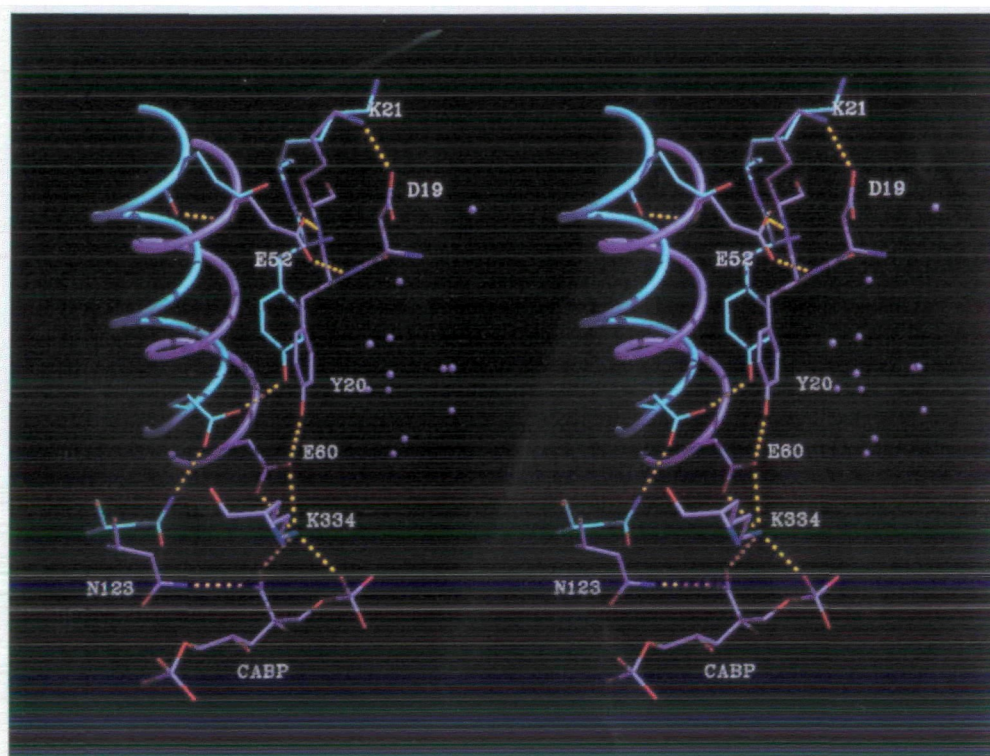


Fig. 2. Stereo view of the structural changes in α -helix B and the N-terminal strand near Lys-21 of the carbamylated and CABP-carbamylated spinach RuBisCO. The main chains and side residues of the carbamylated form and the quaternary complex are shown in cyan and blue, respectively. Oxygen and nitrogen atoms are colored red and dark blue, respectively. Yellow dotted lines represent ionic and hydrogen bonds. Water molecules bound to these regions of the CABP-carbamylated RuBisCO complex are shown as small blue spheres. The carbon skeleton and oxygen atoms of CABP occupying the catalytic site of the neighboring LS are shown in blue and red, respectively. Lys-334 is from the neighboring LS. The structure of the CABP-carbamylated RuBisCO in this figure is the form with an ionic interaction between Lys-21 and Asp-19.

terminal and C-terminal domains. This observation is consistent with previous results that a hydrophobic fluorescent probe attached to the carbamylated enzyme is released from the enzyme along with the slow hysteretic conformational change that occurs after the binding of CABP, RuBP or 6-phosphogluconate to the catalytic sites (19). The failure of the probe to re-bind to RuBisCO once it is released during the RuBP-carboxylation reaction suggests that both the water molecules and the N-terminal domain must be stabilized as they are in the CABP-carbamylated RuBisCO. *Euglena gracilis* RuBisCO possesses arginines at both positions 21 and 305 and shows neither hysteresis nor release of the fluorescence probe during the reaction (19). Thus, the slow binding of water molecules is likely to be involved in the stabilization of the structure with microheterogeneity of spinach RuBisCO.

We propose that the movement of the side chains of Lys-21 and Lys-305 and the subsequent stabilization of these structures by a bond network composed of interactions between amino acid residues and water molecules affect catalysis indirectly. Lys-21 contributes to the network of bonds positioning Lys-334 within the catalytic site in four of the eight LS. In particular, the interaction between α -helix B and Tyr-20 and Lys-21 through Glu-52 and Glu-60 may affect interactions between Glu-60 and Lys-334. A

small rotation of the N-terminal domain toward the catalytic site of the neighboring LS is the driving force in all LS for the large movement of α -helix B toward the catalytic site to construct the catalytic center (23). Lys-305 may also influence the rotation flexibility of the N-terminal domain differently in the two types of LS. The OE1 and OE2 of Glu-60 are 3.06 and 3.13 Å, respectively, away from the NZ of Lys-334 in LS showing the K-D and K-E interactions (Table I). On the other hand, they are 3.03 and 3.10 Å, respectively, away in LS in the free Lys-21 state or showing the K-OXT interaction (Table I). However, in the cyanobacterial enzyme, which shows no hysteresis but a much higher turnover rate than the plant enzyme (4), both carboxyl O are 3.07 Å away from the NZ of Lys-334. In the cyanobacterial RuBisCO, Lys-305 is replaced by arginine

TABLE I. Distance of carboxyl oxygens of Glu-60 from the ϵ -nitrogen of Lys-334 in the two types of LS in spinach RuBisCO.

RuBisCO source	Lys-21	Lys-305	Distance to Lys-334NZ (Å)	
			OE1	OE2
Spinach	K-D	K-E	3.06	3.13
	Free	K-OXT	3.03	3.10
<i>Synechococcus</i>	(E93-R305-L475)		3.07	3.07

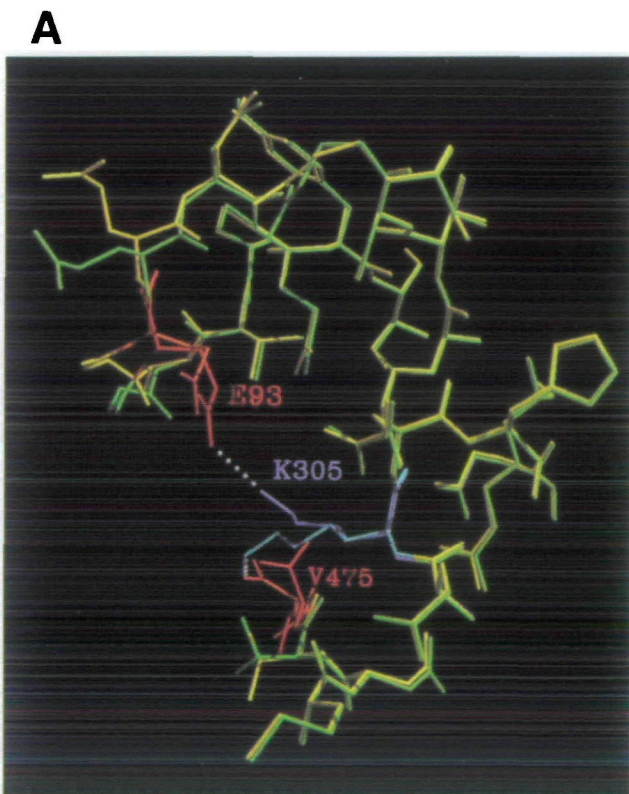
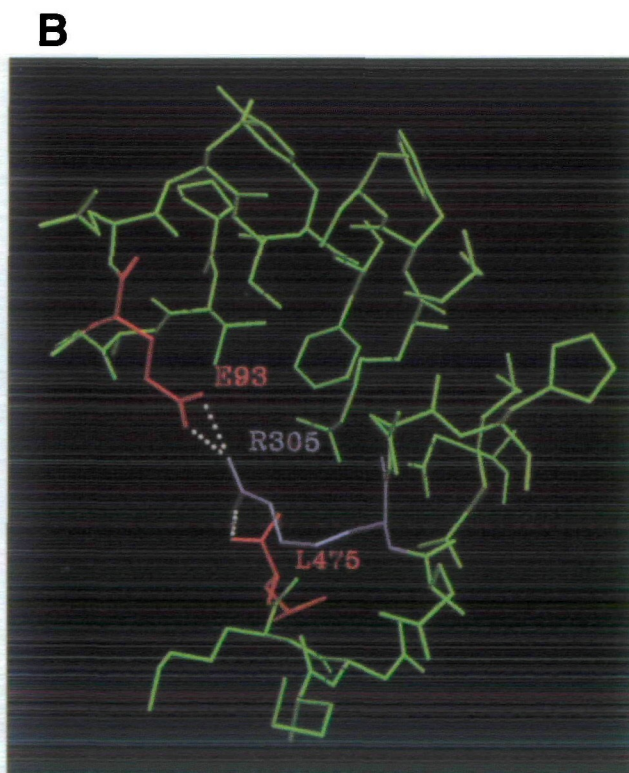


Fig. 3. A: Structural significance of Lys-305 in maintaining the cleft formed between the N-terminal and C-terminal domains of the CABP-carbamylated spinach RuBisCO. The structures of the LS in the K-E and K-OXT states are depicted at the same time. The N-terminal and C-terminal domains of the LS with the K-E interactions are green; those of the LS with the K-OXT interactions are yellow. In the K-E state, residues Glu-93 and Val-475 are red, and residue 305 is blue. These are vermilion and cyan blue, respectively, in the K-OXT state. Note that the K-E bond makes a bridge over the



large cleft formed between the two domains. B: The structure of the corresponding site in the CABP-carbamylated *Synechococcus* RuBisCO (18) showing the simultaneous formation of ion bridges by the guanidyl group of Arg-305 with the carboxyl group oxygens of Glu-93 and the C-terminal carboxyl carbon of Leu-475. The bulk structure is colored green, residues Glu-93 and Leu-475 are red, and residue Arg-305 is colored blue. This figure is depicted in the same orientation as for the spinach enzyme.

(38), which forms ionic bonds with both the carboxyl group of Glu-93 and the C-terminal carboxyl group (Fig. 3B). This may prevent the rotation of the N-terminal domain, keeping Glu-60 closer to Lys-334 and resulting in a high turnover rate. Similarly, *Rhodospirillum rubrum* RuBisCO shows neither hysteresis (39) nor N-terminal domain rotation (40). Thus, the catalytic rate of LS with a free Lys-21 and showing the K-OXT interaction may be greater than LS showing the K-D and K-E interactions due to an effect on the ability of Lys-334 to polarize CO₂, and stabilize the reaction intermediate. The very small difference in the location of Glu-60 between the two types of LS may be important for a change in the catalytic rate without a complete

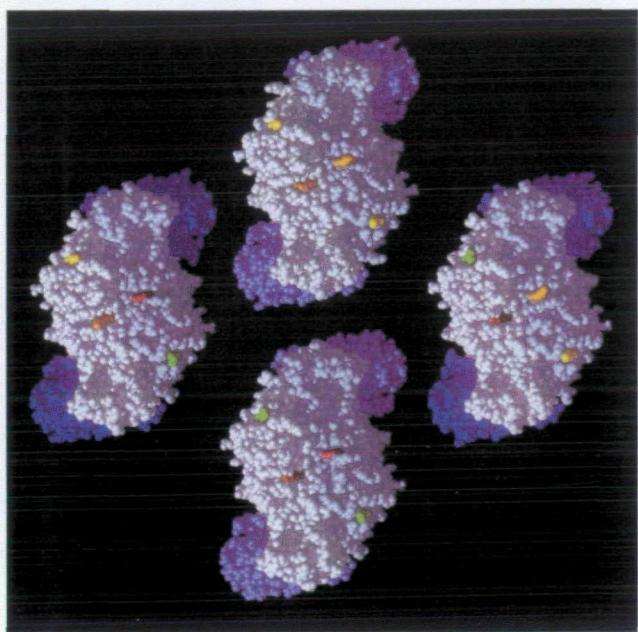


Fig. 4. Overall heterogeneity among subunits in a holoenzyme quaternary complex of spinach RuBisCO. Sphere models colored in white and gray are L2 dimers. Lys-21 and Lys-305 are highlighted in yellow (free Lys-21), green (K-D for Lys-21), orange (K-OXT for Lys-305), and red (K-E for Lys-305). Two kinds of small subunits, S^I and S^{II} (5), are colored in dark blue and blue, respectively.

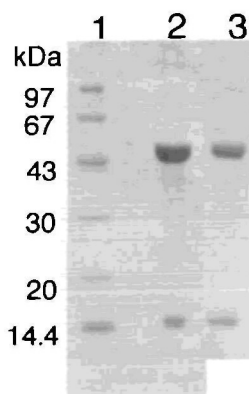


Fig. 5. SDS-PAGE of wild and double-mutated RuBisCO enzymes. SDS-PAGE was done in 12.5% acrylamide gels, and the proteins were visualized by staining with Coomassie Brilliant Blue.

loss of activity, as has been discussed (41).

Introduction of Lys-21 and Lys-305 into *C. vinosum* RuBisCO—The amino acid residues corresponding to Lys-21 and Lys-305 in spinach RuBisCO are arginine and proline in the non-hysteretic RuBisCO of *C. vinosum* (28). The *C. vinosum* RuBisCO is composed of L8S8 and has a high turnover rate. These two arginine and proline residues in the *C. vinosum* RuBisCO were changed to lysines by site-directed mutagenesis. The wild-type (R21/P305) and mutated enzymes (R21K/P305K) were expressed in *E. coli* and purified to homogeneity (numbering of the amino acid residues in *C. vinosum* LS follows that for the spinach enzyme for simple comparison) (Fig. 5). The catalytic sites of wild and mutated RuBisCO in the crude extracts of *E. coli* were measured with a labeled tight-binding transition state analogue, ¹⁴C-CABP. The catalytic number of wild RuBisCO in the crude extract on the basis of the catalytic site was very similar to that of the purified enzyme. On the other hand, the activity of the mutant enzyme increased from 13.8 to 15.8 site⁻¹ s⁻¹ by purification (Table II). This increase was due to the existence of a RuBisCO protein with ¹⁴C-CABP-binding activity but without catalytic activity. In fact, the ¹⁴C-CABP-binding activity was divided into

TABLE II. Some kinetic parameters of *Chromatium* wild and mutant RuBisCOs.

RuBisCO	Crude extract		Purified enzyme	
	<i>k</i> _{cat}	<i>k</i> _{cat}	<i>K</i> _m for CO ₂	Relative specificity
Wild	7.9	8.8	29	44
R21K/P305K	13.5	15.5	241	42

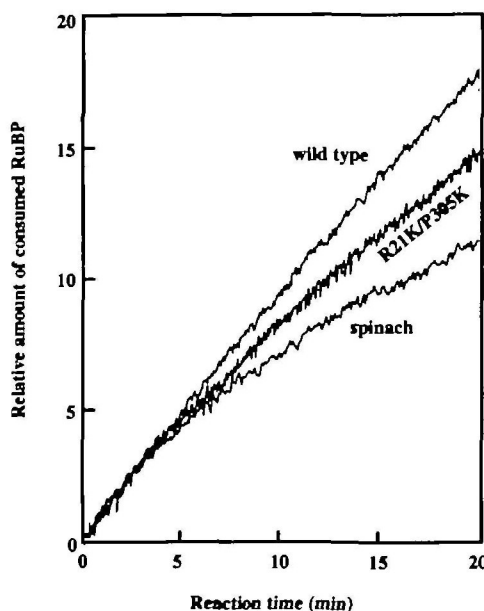


Fig. 6. Courses of the carboxylase reaction with time of the double mutant (R21K/P305K), wild but recombinant (R21/P305), and spinach (K21/K305) RuBisCOs. The protein concentrations were 3, 6, and 15 μg per 3 ml of reaction mixture for R21K/P305K, R21/P305, and K21/K305, respectively. The courses were smoothed once by the spectrogram smoothing system with which the spectrophotometer is equipped. For ease of comparison, relative amounts of RuBP consumed are presented by fixing the amounts consumed in the first one minute at unity.

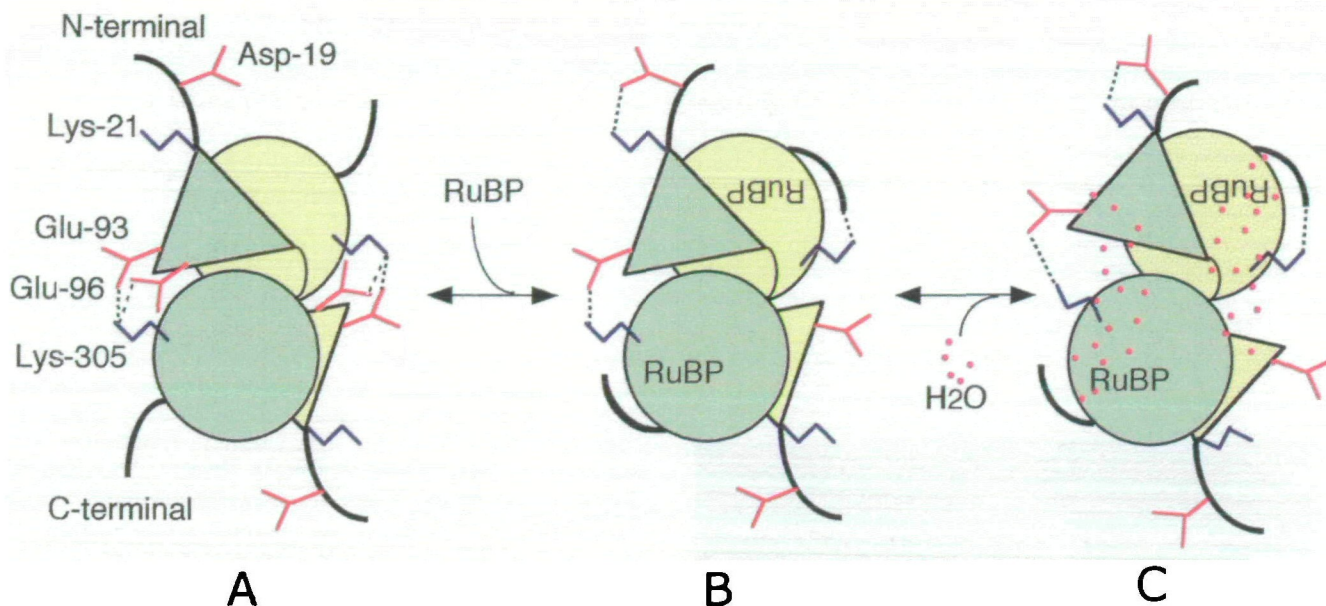


Fig. 7. **Schematic drawing of the fallover mechanism.** The N-terminal and C-terminal domains of one LS are represented by a triangle and a circle, respectively. In an L2 dimer, one LS is colored green and the other is in yellow. Water molecules are depicted by red

dots. Note that in an L2 dimer, one LS shows the K-D/K-E interactions while the other LS shows the free Lys-21 state and the K-OXT interaction. See the text for details.

two fractions by gel filtration on Superdex 200, the void-volume and 500 to 550 kDa fractions. The former fraction showed CABP-binding activity with no CO_2 -fixation activity, while the latter showed both activities. SDS-PAGE of the void-volume fraction revealed a protein band of LS without any SS band (data not shown), although the latter had both subunits (Fig. 5). The latter fractions were used for further analyses.

The course of the carboxylase reaction with the purified mutated and wild-type enzymes was analyzed spectrophotometrically (Fig. 6). The wild-type enzyme exhibited a course that was linear with reaction time. But the R21K/P305K enzyme showed strong hysteresis. The reaction course was virtually linear after the initial decrease. In addition, the kinetic constants for the double mutant (R21K/P305K) were altered (Table II), with the initial k_{cat} increasing from 8.8 to 15.5 $\text{site}^{-1} \text{s}^{-1}$ and the k_{cat} increasing 1.4 times over that of the wild-type enzyme even after hysteresis. Although the relative specificity between the carboxylase and oxygenase reactions was not changed (43.8 in the wild-type enzyme and 41.8 in the mutant enzyme), the Michaelis constant for CO_2 of the double mutant increased to 240 from 33 μM in the wild-type enzyme.

DISCUSSION

Molecular Mechanism of Hysteresis in RuBisCO—The structural and enzymological analyses in this report confirm that Lys-21 and Lys-305 are key residues involved in the hysteresis of RuBisCO. A plausible model for fallover is depicted in Fig. 7. In the carbamylated enzyme, Lys-305 attracts the N-terminal domain through K-2E interactions with Glu-93 and Glu-96, as α -helix B maintains an “open” state (23, 33). Lys-21 does not influence the position of α -helix B because residues 1–19 and the side chain of Lys-21 are free. The C-terminal region of the LS (residues 463–

475) and loop 6 are also free (23).

The binding of RuBP to the catalytic site initiates catalysis in which Loop 6 adopts a “closed” state that serves both to activate the substrate CO_2 via Lys-334 and to stabilize the transition state compound for each turnover (23, 34, 42). α -Helix B and Glu-60 soon slide to the catalytic site to stabilize loop 6. The K-2E interactions are broken and K-D and K-E interactions occur in four LS. The salt bridges formed between α -helix B and residues Asp-19 to Lys-21 (K-D interactions) ensure that Glu-60 is precisely positioned close to Lys-334 as in the *Synechococcus* RuBisCO (Table I). The remaining four LS adopt only K-OXT interactions with free Lys-21. The C-terminal region is also trapped on loop 6 to promote catalysis. These structures may confer on RuBisCO the “high activity” seen just after the initiation of catalysis. Water molecules are incorporated over time around the N-terminal region and into the cleft between the N-terminal and C-terminal domains and the space between the C-terminal region and loop 6. The hydrogen bonds formed between the water molecules and the N-terminal amino acid residues (residues 1 to 21) distance slightly α -helix B and Glu-60 from Lys-334. This distancing is accentuated by the formation of a hydrogen bond between Lys-21 and Asp-19 (K-D interactions) (Table I and Figs. 1 and 2). Consequently, the catalytic activity of LS with the K-D and K-E interactions may be lower than that of LS in the other interaction. These structures will be further stabilized by the hydrogen bonds between the water molecules and the C-terminal region and the cleft. The finding that the removal of Val-475 severely harms catalysis in spinach RuBisCO (43) is well-explained by the present observations. Thus, it is reasoned that the observed high activity before hysteresis is ascribed to a flexible structure of LS and the lower activity after hysteresis is due to a partial loss of activity in four LS with K-D and K-E interactions. In this context, it is interesting to note that

RuBisCO activase eliminates fallover from plant RuBisCO (44, 45) by interacting with a few residues from β -strands C and D (46, 47). These strands further interact with β -strand B to influence the location of Glu-60 (47).

The introduction of hysteresis into the *Chromatium* enzyme clearly demonstrates that the lysine residues are at least two of the amino acid residues involved in hysteresis in spinach RuBisCO. However, the slower gradual inhibition with reaction time observed after the occurrence of hysteresis in spinach RuBisCO (Fig. 5) was not produced by the present double mutation. If the formation of suicide inhibitors during catalysis were the cause of fallover (17, 18), or changes in the two amino acid residues of *C. vinosum* RuBisCO to lysine had changed the bacterial enzyme to an inhibitor-sensitive form, the double-mutated enzyme should have shown a plant-type reaction course. This was not the case (Fig. 6). The reaction of the mutant enzyme showed a bending in the reaction course with time only during the initial few minutes. On the other hand, if a proposed RuBP analogue contaminating the home-made RuBP preparation (48) had become an inhibitor of the double-mutated enzyme but not the wild enzyme, the reaction course of the mutated enzyme with time should have been plant-type. The observed short-term decrease in activity cannot be explained by inhibitors. This supports our previous idea that "fallover" in spinach RuBisCO consists of hysteresis and a slower inhibition by suicide inhibitors (20).

In the present studies, genetic engineering of *C. vinosum* RuBisCO resulted in an enzyme that displayed hysteresis and an altered k_{cat} (Table II). Given the high structural homology among various RuBisCO proteins (24) and the ability of Lys-21 and Lys-305 to influence the reaction rate in spinach RuBisCO, the introduction of these residues into the bacterial enzyme might have affected the catalytic site structures to show a larger k_{cat} than the wild-type enzyme.

While both LS and SS are essential for catalysis in L8S8 RuBisCO enzymes, the SS-depleted L8 octamer of the *Synechococcus* enzyme still binds CABP (49, 50). In this study with the mutated genes of *Chromatium* RuBisCO, some LS existed in a form with the higher molecular mass than the L8S8 form and showing CABP-binding activity in the crude extract of *E. coli*. The occurrence of the SS-less form with CABP-binding activity might have caused the slightly lower measured k_{cat} (Table II).

The present studies increase our understanding of the ways in which individual residues contribute to catalysis. Structural microheterogeneity among subunits with identical amino acid sequences in an enzyme is important for the fine regulation of catalysis, as has been postulated for the allosteric enzyme phosphoglycerate dehydrogenase from *E. coli* (51). Success in increasing k_{cat} in this study and the existence of RuBisCO with a relative specificity over 230 (31) fosters the expectation that we can improve RuBisCO in crop plants and thereby increase productivity.

Entire Architecture of RuBisCO—The protomers of a RuBisCO holoenzyme have been functionally divided into two groups. In binding to the putative regulatory sites of the quaternary complex, CABP binds the first 4 protomers with much higher affinities than those of the remaining protomers (26). A similar phenomenon is observed with RuBP (52) and 6-phosphogluconate (53). Stimulation of the carbamylation of RuBisCO by inorganic phosphate may also occur by the same mechanism, although the exact

inorganic phosphate-binding sites differ from the regulatory sites (54). Structural analyses have not been done for these functional heterogeneities.

Intersubunit structural microheterogeneity has been observed for SS of spinach RuBisCO (9). The eight SS in the RuBisCO holoenzyme are divided into two groups on the basis of their primary structures. His-56 residues in four SS are changed to Leu-56 in the remaining four SS. The two SS types are symmetrically and orderly disposed in the holoenzyme. The imidazol N of His-56 is in ionic interaction with the carbonyl oxygen of Glu-259, the carboxyl oxygen of which participates in an ionic interaction with Arg-258 in the neighboring L2 dimer; this serves, in part, to adhere two L2 dimers together (33). It has been postulated that the eight LS might also be grouped into two categories through this imidazol function and that this interaction may be involved in the functional cooperativity of the binding of sugar phosphates on the putative regulatory sites (9). The intersubunit microheterogeneity with respect to Lys-21 and Lys-305 also groups the eight LS into two classes; these may correspond to high- and low-activity LS (Table I). Both types of LS are carbamylated and catalyze the carboxylation of RuBP, but their turnover rates may be very different due to a small change in the location of the α -amino group of Lys-334.

Considering these and our previous results, RuBisCO may function as a complex formed from four dimers, each of which has two-types of protomers with different properties. This will give rise to cooperativity in binding of sugar phosphates to the regulatory sites and hysteresis in catalysis. Examining the functional significance of the interaction between SS heterogeneity and intersubunit microheterogeneity of LS (Fig. 4) is our next interest.

The authors thank Drs. M.A.J. Parry, S. Rodermeil, A. Kaplan, and H.J. Bohnert for reviewing the paper before submission. We also thank Drs. A. Kaplan, G.H. Lorimer, and L. Bogorad for their discussion in the Super-RuBisCO project as project members and Dra. I. Andersson (spinach RuBisCO) and C.-I. Branden and S. Gutteridge (cyanobacterial RuBisCO) for supplying the structural coordinates for these enzymes.

REFERENCES

1. von Caemmerer, S. and Farquhar, G.D. (1981) Some relationships between the biochemistry of photosynthesis and the gas exchange of leaves. *Planta* **153**, 376–387
2. Makino, A., Mae, T., and Ohira, K. (1985) Photosynthesis and ribulose-1,5-bisphosphate carboxylase/oxygenase in rice (*Oryza sativa*) leaves from emergence through senescence: Quantitative analysis by carboxylation/oxygenation and regeneration of ribulose 1,5-bisphosphate. *Plant Physiol.* **79**, 57–61
3. Woodlow, I.E. and Berry, J.A. (1988) Enzymatic regulation of photosynthetic CO₂ fixation in C3 plants. *Annu. Rev. Plant Physiol. Plant Mol. Biol.* **39**, 533–594
4. Andrews, T.J. and Lorimer, G.H. (1987) Rubisco: structure, mechanisms, and prospects for improvement in *Biochemistry of Plants*, Vol. 10 (Hatch, M.D. and Boardman, N.K., eds.) pp. 131–218, Academic Press, New York
5. Schneider, G., Lindqvist, Y., and Branden, C.-I. (1992) RUBISCO: structure and mechanism. *Annu. Rev. Biophys. Biomol. Struct.* **21**, 119–143
6. Spreitzer, R.J. (1993) Genetic dissection of rubisco structure and function. *Annu. Rev. Plant Physiol. Plant Mol. Biol.* **44**, 411–434
7. Hartman, F.C. and Harpel, M.R. (1994) Structure, function,

- regulation, and assembly of D-ribulose-1,5-bisphosphate carboxylase/oxygenase. *Annu. Rev. Biochem.* **63**, 197–234
8. Manzara, T. and Grussem, W. (1988) Organization and expression of the genes encoding ribulose-1,5-phosphate carboxylase in higher plants. *Photosynth. Res.* **16**, 117–139
 9. Shibata, N., Inoue, T., Fukuhara, K., Nagara, Y., Kitagawa, R., Harada, S., Kasai, N., Uemura, K., Kato, K., Yokota, A., and Kai, Y. (1996) Orderly disposition of heterogeneous small subunits in *d*-ribulose-1,5-bisphosphate carboxylase/oxygenase from spinach. *J. Biol. Chem.* **271**, 26449–26452
 10. Jordan, D.B. and Ogren, W.L. (1980) Species variation in the specificity of ribulose bisphosphate carboxylase/oxygenase. *Nature* **291**, 513–515
 11. Jordan, D.B. and Ogren, W.L. (1983) Species variation in kinetic properties of ribulose 1,5-bisphosphate carboxylase/oxygenase. *Arch. Biochem. Biophys.* **227**, 425–433
 12. Uemura, K., Suzuki, Y., Shikanai, T., Wadano, A., Jensen, R.G., Chmara, W., and Yokota, A. (1996) A rapid and sensitive method for determination of relative specificity of RuBisCO from various species by anion-exchange chromatography. *Plant Cell Physiol.* **37**, 325–331
 13. Seemann, J.A., Badger, M.R., and Berry, J.A. (1984) Variations in the specific activity of ribulose-1,5-bisphosphate carboxylase between species utilizing differing photosynthetic pathways. *Plant Physiol.* **74**, 791–794
 14. Jensen, R.G. and Bahr, T.J. (1977) Ribulose 1,5-bisphosphate carboxylase/oxygenase. *Annu. Rev. Plant Physiol.* **28**, 379–408
 15. Robinson, S.P. and Portis, A.R., Jr. (1989) Ribulose 1,5-bisphosphate carboxylase/oxygenase activase protein prevents the *in vitro* decline in activity of ribulose-1,5-bisphosphate carboxylase/oxygenase. *Plant Physiol.* **90**, 968–971
 16. Yokota, A. and Kitaoka, S. (1989) Linearity and functioning forms in the carboxylase reaction of spinach ribulose 1,5-bisphosphate carboxylase/oxygenase. *Plant Cell Physiol.* **30**, 183–191
 17. Edmondson, D.L., Badger, M.R., and Andrews, T.J. (1990) A kinetic characterization of slow inhibition of ribulose bisphosphate carboxylase during catalysis. *Plant Physiol.* **93**, 1376–1382
 18. Zhu, G. and Jensen, R.G. (1991) Fallover of ribulose 1,5-bisphosphate carboxylase/oxygenase activity. *Plant Physiol.* **97**, 1348–1353
 19. Yokota, A. (1991) Ribulose bisphosphate-induced, slow conformational changes of spinach ribulose bisphosphate carboxylase cause the two types of inflections in the course of its carboxylation reaction. *J. Biochem.* **110**, 246–252
 20. Yokota, A., Wadano, A., and Murayama, H. (1996) Modeling of continuously and directly analyzed biphasic reaction courses of ribulose 1,5-bisphosphate carboxylase/oxygenase. *J. Biochem.* **119**, 487–499
 21. Edmondson, D.L., Badger, M.R., and Andrews, T.J. (1990) Slow inactivation of ribulose bisphosphate carboxylase is caused by accumulation of low, tight-binding inhibitor at the catalytic site. *Plant Physiol.* **93**, 1390–1397
 22. Yokota, A. and Tokai, H. (1993) Lysine residues involved in the hysteresis and in the regulatory sites of spinach ribulose 1,5-bisphosphate carboxylase/oxygenase. *J. Biochem.* **114**, 746–753
 23. Taylor, T.C. and Andersson, I. (1996) Structural transitions during activation and ligand binding in hexadecameric Rubisco inferred from the crystal structure of the activated unliganded spinach enzyme. *Nature Struct. Biol.* **3**, 95–101
 24. Newman, J. and Gutteridge, S. (1993) The x-ray structure of *Synechococcus* ribulose-bisphosphate carboxylase/oxygenase-activated quaternary complex at 2.2 Å resolution. *J. Biol. Chem.* **268**, 25876–25886
 25. Newman, J., Branden, C.-I., and Jones, A. (1993) Structure determination and refinement of ribulose 1,5-bisphosphate carboxylase/oxygenase from *Synechococcus* PCC6301. *Acta Crystallogr. Sec. D* **49**, 548–560
 26. Yokota, A., Higashioka, M., and Wadano, A. (1991) Cooperative binding of carboxyarabinitol bisphosphate to the regulatory sites of ribulose bisphosphate carboxylase/oxygenase from spinach. *J. Biochem.* **110**, 253–256
 27. Ito, W., Ishiguro, H., and Kurosawa, Y. (1991) A general method for introducing a series of mutations into cloned DNA using the polymerase chain reaction. *Gene* **102**, 67–70
 28. Viale, A.M., Kobayashi, H., and Akazawa, T. (1989) Expressed genes for plant-type ribulose 1,5-bisphosphate carboxylase/oxygenase in the photosynthetic bacterium *Chromatium vinosum*, which possesses two complete sets of the genes. *J. Bacteriol.* **171**, 2391–2400
 29. Viale, A.M., Kobayashi, H., and Akazawa, T. (1990) Distinct properties of *Escherichia coli* products of plant-type ribulose-1,5-bisphosphate carboxylase/oxygenase directed by two sets of genes from the photosynthetic bacterium *Chromatium vinosum*. *J. Biol. Chem.* **265**, 18386–18392
 30. Laemmli, U.K. (1970) Cleavage of structural proteins during the assembly of the head of bacteriophage T4. *Nature* **227**, 680–685
 31. Uemura, K., Anwaruzzaman, Miyachi, S., and Yokota, A. (1997) Ribulose-1,5-bisphosphate carboxylase/oxygenase from thermophilic red algae with a strong specificity for CO₂ fixation. *Biochem. Biophys. Res. Commun.* **233**, 568–571
 32. Bradford, M.M. (1976) A rapid and sensitive method for the quantification of microgram quantities of protein utilizing the principle of protein-dye binding. *Anal. Biochem.* **72**, 248–254
 33. Knight, S., Andersson, I., and Branden, C.-I. (1990) Crystallographic analysis of ribulose 1,5-bisphosphate carboxylase from spinach at 2.4 Å resolution: subunits interactions and the active site. *J. Mol. Biol.* **215**, 113–160
 34. Andersson, I. (1996) Large structures at high resolution: The 1.6 Å crystal structure of spinach ribulose-1,5-bisphosphate carboxylase/oxygenase complexed with 2-carboxyarabinitol bisphosphate. *J. Mol. Biol.* **259**, 160–174
 35. Lorimer, G.H., Chen, Y.-R., and Hartman, F.C. (1993) A role for the ε-amino group of lysine-334 of ribulose-1,5-bisphosphate carboxylase in the addition of carbon dioxide to the 2,3-enediol(ate) of ribulose-1,5-bisphosphate. *Biochemistry* **32**, 9018–9024
 36. Ferrin, T.E., Huang, C.C., Jarvis, L.E., and Langridge, R. (1988) The MIDAS display system. *J. Mol. Graphics* **6**, 13–27
 37. Huang, C.C., Pettersen, T.E., Klein, T.E., Ferrin, T.E., and Langridge, R. (1991) Conic: a fast renderer for space-filling molecules with shadows. *J. Mol. Graphics* **9**, 230–236
 38. Shinozaki, K., Yamada, C., Takahata, N., and Sugiura, M. (1983) Molecular cloning and sequence analysis of the cyanobacterial gene for the large subunit of ribulose-1,5-bisphosphate carboxylase/oxygenase. *Proc. Natl. Acad. Sci. USA* **80**, 4050–4054
 39. Lee, E.N., Harpel, M.R., Chen, Y.R., and Hartman, F.C. (1993) Perturbation of reaction intermediate partitioning by a site-directed mutant of ribulose-bisphosphate carboxylase/oxygenase. *J. Biol. Chem.* **268**, 26583–26591
 40. Lundqvist, T. and Schneider, G. (1989) Crystal structure of the complex of ribulose-1,5-bisphosphate carboxylase and a transition state analogue, 2-carboxy-D-arabinitol 1,5-bisphosphate. *J. Biol. Chem.* **264**, 7078–7083
 41. Spreitzer, R.J., Thow, G., and Zhu, G. (1995) Pseudoreversion substitution of large-subunit residue 54 influences the CO₂/O₂ specificity of chloroplast ribulose-bisphosphate carboxylase/oxygenase. *Plant Physiol.* **109**, 681–685
 42. Schneider, G., Lindqvist, Y., and Lundqvist, T. (1990) Crystallographic refinement and structure of ribulose-1,5-bisphosphate carboxylase from *Rhodospirillum rubrum* at 1.7 Å resolution. *J. Mol. Biol.* **211**, 989–1008
 43. Portis, A.R., Jr. (1990) Partial reduction in ribulose 1,5-bisphosphate carboxylase/oxygenase activity by carboxypeptidase A. *Arch. Biochem. Biophys.* **283**, 397–400
 44. Robinson, S.P. and Portis, A.R., Jr. (1989) Ribulose 1,5-bisphosphate carboxylase/oxygenase activase protein prevents the *in vitro* decline in activity of ribulose 1,5-bisphosphate carboxylase/oxygenase. *Plant Physiol.* **90**, 968–971
 45. Yokota, A. and Tsujimoto, N. (1992) Characterization of ribulose-1,5-bisphosphate carboxylase/oxygenase carrying ribulose

- 1,5-bisphosphate at its regulatory sites and the mechanism of interaction of this form of the enzyme with ribulose-1,5-bisphosphate-carboxylase/oxygenase activase. *Eur. J. Biochem.* **204**, 901–909
46. Larson, E.M., O'Brien, C.M., Zhu, G., Spreitzer, R.J., and Portis, A.R., Jr. (1997) Specificity for activase is changed by a Pro-89 to Arg substitution in the large subunit of ribulose-1,5-bisphosphate carboxylase/oxygenase. *J. Biol. Chem.* **272**, 17033–17037
47. Ott, C.M., Smith, B.D., Portis, A.R., and Spreitzer, R.J. (2000) Activase region on chloroplast ribulose-1,5-bisphosphate carboxylase/oxygenase: nonconservative substitution in the large subunit alters species specificity of protein interaction. *J. Biol. Chem.* **275**, 26241–26244
48. Kane, H.J., Wilkin, J.-M., Portis, A.R., Jr., and Andrews, T.J. (1998) Potent inhibition of ribulose-bisphosphate carboxylase by an oxidized impurity in ribulose-1,5-bisphosphate. *Plant Physiol.* **117**, 1059–1069
49. Andrews, T.J., Lorimer, G.H., and Pierce, J. (1986) Three partial reactions of ribulose-bisphosphate carboxylase require both large and small subunits. *J. Biol. Chem.* **261**, 12184–12188
50. Andrews, T.J. (1988) Catalysis of cyanobacterial ribulose-bisphosphate carboxylase large subunits in the complete absence of small subunits. *J. Biol. Chem.* **263**, 12213–12219
51. Schuller, D.J., Grant, G.A., and Banaszak, L.J. (1995) The allosteric ligand site in the V_{max} -type cooperative enzyme phosphoglycerate dehydrogenase. *Nat. Struct. Biol.* **2**, 69–76
52. Yokota, A., Higashioka, M., Taira, T., Usuda, H., Wadano, A., and Murayama, H. (1994) Binding of ribulose 1,5-bisphosphate to the non-catalytic sites of ribulose 1,5-bisphosphate carboxylase/oxygenase and its metabolic implication. *Plant Cell Physiol.* **35**, 317–321
53. Yokota, A., Higashioka, M., and Wadano, A. (1992) Regulation of the activity of ribulose-1,5-bisphosphate carboxylase/oxygenase through cooperative binding of 6-phosphogluconate to its regulatory sites. *Eur. J. Biochem.* **208**, 721–727
54. Anwaruzzaman, Sawada, S., Usuda, H., and Yokota, A. (1995) Regulation of ribulose 1,5-bisphosphate carboxylase/oxygenase activation by inorganic phosphate through stimulating the binding of the activator CO_2 to the activation sites. *Plant Cell Physiol.* **36**, 425–433